



THE UNIVERSITY *of* EDINBURGH

Edinburgh Research Explorer

Solubility trapping in formation water as dominant CO₂ sink in natural gas fields

Citation for published version:

Gilfillan, SMV, Lollar, BS, Holland, G, Blagburn, D, Stevens, S, Schoell, M, Cassidy, M, Ding, Z, Zhou, Z, Lacrampe-Couloume, G & Ballentine, CJ 2009, 'Solubility trapping in formation water as dominant CO₂ sink in natural gas fields', *Nature*, vol. 458, no. 7238, pp. 614-618. <https://doi.org/10.1038/nature07852>

Digital Object Identifier (DOI):

[10.1038/nature07852](https://doi.org/10.1038/nature07852)

Link:

[Link to publication record in Edinburgh Research Explorer](#)

Document Version:

Peer reviewed version

Published In:

Nature

Publisher Rights Statement:

The final version of this work was published in Nature copyright of the Nature Publishing Group (2009) available online

General rights

Copyright for the publications made accessible via the Edinburgh Research Explorer is retained by the author(s) and / or other copyright owners and it is a condition of accessing these publications that users recognise and abide by the legal requirements associated with these rights.

Take down policy

The University of Edinburgh has made every reasonable effort to ensure that Edinburgh Research Explorer content complies with UK legislation. If you believe that the public display of this file breaches copyright please contact openaccess@ed.ac.uk providing details, and we will remove access to the work immediately and investigate your claim.



This is the author final draft or 'post-print' version made available through Edinburgh Research Explorer. The final version was published in Nature copyright of the Nature Publishing Group (2009)

Cite As: Gilfillan, SMV, Lollar, BS, Holland, G, Blagburn, D, Stevens, S, Schoell, M, Cassidy, M, Ding, Z, Zhou, Z, Lacrampe-Couloume, G & Ballentine, CJ 2009, 'Solubility trapping in formation water as dominant CO₂ sink in natural gas fields' *Nature*, vol 458, no. 7238, pp. 614-618.

DOI: 10.1038/nature07852

Solubility trapping in formation water as dominant CO₂ sink in natural gas fields

Stuart M. V. Gilfillan*, Barbara Sherwood Lollar, Greg Holland, Dave Blagburn, Scott Stevens, Martin Schoell, Martin Cassidy, Zhenju Ding, Zheng Zhou, Georges Lacrampe-Couloume and Chris J. Ballentine

*Author to whom correspondence should be addressed:

Scottish Carbon Capture and Storage, School of GeoSciences, The University of Edinburgh, Grant Institute, The King's Buildings, West Mains Road, Edinburgh, EH9 3JW, UK.

Email: stuart.gilfillan@ed.ac.uk

Injecting CO₂ into deep geological strata is proposed as a safe and economically favourable means to store CO₂ captured from industrial point sources¹⁻³. However, it is difficult to assess the long term consequence of CO₂ flooding in the subsurface from decadal observations of existing disposal sites^{1,2}. Both the site design and long term safety modelling critically depend on how and where CO₂ will be stored in the site over its lifetime²⁻⁴. Natural gas fields dominated by a CO₂ phase provide an essential natural analogue for assessing the safety and viability of the geological storage of anthropogenic CO₂ over millennia timescales^{1,2,5,6}. Here, we show that the dominant subsurface sink of CO₂ in nine natural gas fields from North America, China and Europe is through dissolution (solubility trapping) in the formation water. All fields, whether siliciclastic or carbonate dominated reservoir lithologies, exhibit a reduction in CO₂ relative to ³He, an inert and highly insoluble tracer that correlates with an increase in formation water-derived noble gases. Reservoir CO₂ phase loss, sometimes > 90% of that emplaced, is therefore quantitatively related to formation water involvement in the system. CO₂/³He and δ¹³C(CO₂) data for seven gas fields indicate that dissolution in formation water at pH=5-5.8 alone is the major sink for the CO₂ loss. Within two siliciclastic dominated reservoirs some CO₂ loss through precipitation as carbonate minerals cannot be ruled out, but may account for a maximum of 18% loss of the emplaced CO₂. Long term anthropogenic CO₂ storage models in similar geological systems must consider the potential mobility of CO₂ dissolved in water and not geological mineral fixation, which is an insignificant CO₂ trapping mechanism.

Noble gas and CO₂ carbon isotopes are powerful tracers of crustal fluid processes that act on subsurface CO₂^{5,7-10}. Within a geological storage site, CO₂ injected as a free CO₂ phase (gas or supercritical) may over time be dissolved in solution (solubility trapping), or locked within carbonate minerals by precipitation (mineral trapping)^{4,11}. By using noble gas and carbon

isotope tracers together to study naturally occurring CO₂ systems, we can uniquely identify and quantify the principal mechanism of the CO₂ phase removal, mineral or solubility trapping, over a time scale not accessible through extant injection studies.

We combine noble gas data from five natural CO₂ reservoirs located within the Colorado Plateau and Rocky Mountain provinces, (McCallum Dome, Sheep Mountain, McElmo Dome, CO., Bravo Dome, NM, and St Johns Dome, AZ.)⁷ with new $\delta^{13}\text{C}(\text{CO}_2)$ isotope data (Table 1). Previous work has shown that noble gas patterns in these gas fields are explained by CO₂ gas stripping of the formation water during reservoir filling, followed by partial dissolution of noble gases back into the formation water⁷. We also consider published noble gas and stable isotope information in a further four CO₂-rich natural gas fields (JM-Brown Bassett field (JMBB), Permian Basin, Texas⁵; Kismarja field, Pannonian Basin, Hungary⁸; Jilin field, Jilin Province, Songliao Basin; and Subei Basin field, Jiangsu Province in China^{12,13}).

CO₂/³He ratios within the magmatic range of 1-10x10⁹ have been used to identify a primary magmatic origin of the CO₂ contained within five natural CO₂ reservoirs of the Colorado Plateau and Rocky Mountain Provinces⁷. CO₂/³He within the Subei Basin and JM-Brown Bassett field also indicate a magmatic origin, whilst the CO₂/³He values within the Jilin and Kismarja fields are far higher, suggesting a predominantly crustal origin^{5,8}. All of the reservoirs exhibit local variation in the CO₂ content relative to the inert tracer ³He. As there is not a significant source of ³He within the crust¹⁴, and as ³He is inert and highly insoluble⁹, this variation must be due to changes in the CO₂ component within the reservoirs. While many sources and sinks of CO₂ exist in the subsurface^{4,8,9} we argue later that the CO₂/³He variation is caused by CO₂ loss from the reservoir. The difference between the highest CO₂/³He and lower values can provide a minimum estimate of this CO₂ loss. In the case of Bravo Dome, a reduction of CO₂/³He values from 4.82x10⁹ (BD11) to 2.25x10⁹ (BD02)

indicates a >50% loss of the original CO₂ charge in the portion of the reservoir represented by BD02 (Table 1). McElmo Dome samples exhibit a decrease from 8.5x10⁹ (YD-1) to 0.68x10⁹ (He-2) suggesting >90% emplaced CO₂ loss in portions of this field.

⁴He is continually produced in the subsurface by the radiogenic decay of U, Th and K¹⁴. ²⁰Ne is introduced into the subsurface as a component of air dissolved in water and, as such, can only enter the reservoir system via interaction with formation water⁹. While there is no *a-priori* reason to expect a correlation between ⁴He and ²⁰Ne, this has been observed in natural gases on a regional scale¹⁵. This correlation is the result of ⁴He accumulating in the formation water¹⁶ which also contains atmosphere derived ²⁰Ne, and subsequent quantitative partitioning of both ⁴He and ²⁰Ne into the reservoir phase^{7,15}. Almost all CO₂ reservoirs for which we have ²⁰Ne and ⁴He concentration data show a local ²⁰Ne correlation with ⁴He (Table 1 and supplementary information). A decrease in CO₂/³He is also correlated with ²⁰Ne in most CO₂ reservoirs (Fig. 1) and with ⁴He in all CO₂ reservoirs (Fig. 2).

While there are various mechanisms to add crustal CO₂ (CO₂/³He >> 10¹⁰) to these systems^{4,10} there is no plausible mechanism that enables crustal CO₂ to be variably added to these systems while preserving a correlation of CO₂/³He with the formation water-derived noble gases. Neglecting small amounts of ³He dissolution back into the formation water⁷, changes in CO₂/³He must therefore be due to CO₂ loss in the subsurface via a mechanism directly proportional to the amount of formation water that has been degassed. CO₂ is soluble and reactive. The most likely subsurface CO₂ phase removal mechanisms are solubility and mineral trapping^{4,11}.

Reservoir lithology may exert a significant influence on how changes in CO₂/³He relate to δ¹³C(CO₂). The carbonate reservoirs (McElmo, JMBB, and St. Johns Domes) show little variance in δ¹³C(CO₂) whilst the silicilastic fields (Jilin field, Subei Basin, Kismarja, Sheep

Mountain, McCallum and Bravo Domes) exhibit a greater range in $\delta^{13}\text{C}(\text{CO}_2)$ (Table 1, Supplementary Fig. S1). We consider Bravo and McElmo Domes as case types for each reservoir lithology.

Emplacement of CO_2 at Bravo Dome is believed to have occurred relatively recently (local volcanic activity dates from 8,000-10,000 years)^{7,17} and the field may still be undergoing active CO_2 recharge¹¹. Decreasing $\text{CO}_2/{}^3\text{He}$ within Bravo Dome correlates with more negative $\delta^{13}\text{C}(\text{CO}_2)$ (Fig. 3a). Taking the highest $\text{CO}_2/{}^3\text{He}$ of 4.82×10^9 (BD11) to be the sample that experienced the least CO_2 loss, we calculate the coherent change in $\text{CO}_2/{}^3\text{He}$ and $\delta^{13}\text{C}(\text{CO}_2)$ predicted for CO_2 dissolution into the formation water at various pH and for CO_2 precipitation as a carbonate (see Methods Summary). The data are not consistent with precipitation as carbonate being a major sink for CO_2 at Bravo Dome (Figure 3a). However, while a significant number of the data points are consistent with CO_2 dissolution into formation water at a pH between 6-7, it is not possible to rule out a degree of CO_2 loss due to precipitation together with CO_2 dissolution at a lower pH (e.g. pH=5). In such a two process model an upper limit to the proportion of CO_2 lost to precipitation of approximately 18%, can be attributed (Fig. 3a). Hence, in all cases the major CO_2 sink is dissolution. In situ precipitation of 18% reservoir CO_2 would generate between 3.2-6.1% by mass of the whole rock, dependent on whether dolomite, calcite or dawsonite precipitation was favoured by the reservoir conditions. Whilst evidence for CO_2 rich formation water interaction within the reservoir has been documented, to date no secondary carbonate has been identified¹⁸. Nevertheless, the volume control of the water suggests that the location of the precipitate, if any, is likely to be within the water leg which was not sampled. Lack of reservoir secondary mineralization cannot at this stage rule out any carbonate precipitation as a minor CO_2 sink.

Similar to Bravo Dome, while many of the Sheep Mountain data can be accounted for by dissolution of CO₂ (at pH=5 in this case), a small component of precipitation cannot be ruled out. Adopting the same approach as Bravo Dome, the remaining Sheep Mountain data require a maximum of 10% precipitation and 20% dissolution of the original CO₂ charge (Table 1; Supplementary Fig. S2). In contrast, while minor data scatter may also be due to some small amount of CO₂ precipitation or dissolution at pH=7-8, almost all the data from the other siliciclastic fields of McCallum Dome, Subei basin, Kismarja and the Jilin field can be described by dissolution in the formation water only, within a narrow pH range of between 5-5.3 (Supplementary Figs S3-6).

McElmo Dome carbonate reservoir data show over an order of magnitude change in CO₂/³He with invariant $\delta^{13}\text{C}(\text{CO}_2)$ (Figure 3b). This pattern is repeated in the two other carbonate-dominated fields (Supplementary Figures S7, S8). Invariant $\delta^{13}\text{C}(\text{CO}_2)$ in these fields allows us to discount a two process model of precipitation and dissolution such as at Bravo Dome (Fig. 3a). All data are consistent with CO₂ dissolution into formation water in the pH range of 5.4-5.8 (Figure 3b, Supplementary Figures 7,8), a value similar to the pH obtained for the siliciclastic reservoirs and to values observed (pH=5.7) in carbonate mineral buffered formation water observed in the recent Frio CO₂ injection studies on CO₂ breakthrough¹⁹.

On a reservoir engineering timescale, the early stages of CO₂ injection can result in a drop in pH and dissolution of carbonate minerals into the formation water^{18,20-22}. Any significant CO₂ contribution to the reservoir CO₂ phase from re-dissolution of carbonates would be ³He-free and therefore perturb the CO₂/³He correlation with ⁴He and ²⁰Ne. As there is a clear correlation between CO₂/³He and ⁴He in all fields and ²⁰Ne within the majority, we conclude that dissolution of carbonate minerals into the formation water cannot have had a major influence on $\delta^{13}\text{C}(\text{CO}_2)$ values. There is no evidence for any precipitation of CO₂ within the

carbonate dominated reservoirs, requiring that the dominant mechanism of reservoir CO₂ loss, up to 90%, is through dissolution into the formation water.

Even the most conservative model we have presented places an upper limit on the CO₂ removed by precipitation at approximately 18%, and then only in some samples, from all natural gas fields investigated in a variety of lithological settings. Precipitation of CO₂ over millennial timescales represents at most only a small subsurface trapping mechanism for CO₂, and then only within siliciclastic lithologies. The dominant mechanism of CO₂ loss from most CO₂ natural gas fields can be accounted for through simple dissolution into the formation groundwater within a narrow pH window (pH=5-5.8). This study underscores that geological carbon storage requires careful investigation of existing geologic and hydrogeologic analogues that have naturally accumulated and stored CO₂ over timescales relevant to anthropogenic CO₂ storage facilities. We further demonstrate a means of testing trapping and storage mechanisms via coupled noble gas and carbon isotope measurements in the context of formation/reservoir water pH evolution.

Methods Summary

Detailed descriptions of the sample collection and analysis procedures can be found in the original references^{5,7,8,21,23}. In our calculations (Figure 3 and Supplemental Figures) we use the highest CO₂/³He ratio measured in each field as a reference point to calculate the correlated reservoir CO₂/³He and $\delta^{13}\text{C}(\text{CO}_2)$ ratios as the CO₂ phase is removed by either precipitation or dissolution. We assume open system loss. In the case of precipitation there is zero ³He loss from the CO₂ phase and CO₂/³He changes in proportion to the fraction of the remaining CO₂ phase (f). In the case of dissolution the change in CO₂/³He is calculated following the Rayleigh equation.

Changes in $\delta^{13}\text{C}(\text{CO}_2)$ are calculated using the Rayleigh fractionation equation expressed as:

$$\delta^{13}\text{C}(\text{CO}_2) = \delta^{13}\text{C}(\text{CO}_2)_0 + \epsilon \ln(f) \quad ^{24}$$

where $\delta^{13}\text{C}(\text{CO}_2)_0$ is the original system value, f is the fraction of CO_2 remaining in the reservoir, and ϵ is the carbon isotope fractionation, either for precipitation or for dissolution.

Carbon isotope fractionation factors (α) are calculated as a function of temperature for

$\text{CO}_2(\text{g})$ precipitating to form $\text{CaCO}_3(\text{s})$, or dissolving to form either $\text{H}_2\text{CO}_3(\text{aq})$ or HCO_3^-

(aq) ²⁵. Since all the fractionations are small the simplification can be made that $\epsilon =$

$1000\ln(\alpha)$ ²⁶. For typical reservoir waters of pH range 5-8, the contribution of $\text{CO}_3^{2-}(\text{aq})$ is

negligible. Hence for CO_2 dissolution, carbon isotope fractionation between the dissolved

inorganic carbon (DIC) pool and CO_2 gas used in the Rayleigh fractionation equation can be

expressed as:

$$\epsilon^{13}\text{C}_{\text{DIC-CO}_2(\text{g})} = x(\epsilon^{13}\text{C}_{\text{H}_2\text{CO}_3(\text{aq})-\text{CO}_2(\text{g})}) + (1-x)(\epsilon^{13}\text{C}_{\text{HCO}_3^-(\text{aq})-\text{CO}_2(\text{g})}) \quad ^{24}$$

where x is the proportion of CO_2 gas dissolving to $\text{H}_2\text{CO}_3(\text{aq})$ at the relevant pH²⁴.

Solubility as a function of temperature and salinity is given by the IUPAC solubility series

for CO_2 ²⁷ and by Crovetto et al. and Smith for He^{28,29}. The average well depth, reservoir

pressure, temperature and salinity are presented in the supplementary information for each

reservoir, with the corresponding Henry's Law constants K_{He} , K_{CO_2} , and fractionation factor

$(1000\ln\alpha)$ for $\text{CO}_2(\text{g})$ forming $\text{H}_2\text{CO}_3(\text{aq})$, $\text{HCO}_3^-(\text{aq})$ and $\text{CaCO}_3(\text{s})$ (Supplementary Table 1).

References

- 1 Schrag, D. P. Preparing to Capture Carbon. *Science* **315**, 812-813 (2007).
- 2 Baines, S. J. & Worden, R. H. in *Geological storage of carbon dioxide* Vol. Special Publication 233 (eds S. J. Baines & R. H. Worden) 1-6 (The Geological Society of London, 2004).
- 3 Gale, J. in *Geological Storage of Carbon Dioxide* Vol. 233 *Special Publications* (eds S.J. Baines & R.H. Worden) 7-15 (Geological Society, 2004).
- 4 Bradshaw, J., Boreham, C. & La Pedalina, F. in *Greenhouse Gas Control Technologies, 7th International Conference on Greenhouse Gas Control Technologies* Vol. 1 (eds E. Rubin, D. Keith, & C. Gilboy) 541-550 (Vancouver, 2004).

- 5 Ballentine, C. J., Schoell, M., Coleman, D. & Cain, B. A. 300-Myr-old magmatic CO₂ in natural gas reservoirs of the west Texas Permian basin. *Nature* **409**, 327-331 (2001).
- 6 Kintisch, E. The Greening of Synfuels. *Science* **320**, 306-308 (2008).
- 7 Gilfillan, S. M. V. *et al.* The noble gas geochemistry of natural CO₂ gas reservoirs from the Colorado Plateau and Rocky Mountain provinces, USA. *Geochimica et Cosmochimica Acta* **72**, 1174-1198 (2008).
- 8 Sherwood Lollar, B., Ballentine, C. J. & O'Nions, R. K. The fate of mantle-derived carbon in a continental sedimentary basin: Integration of C/He relationships and stable isotope signatures. *Geochimica et Cosmochimica Acta* **61**, 2295-2308 (1997).
- 9 Ballentine, C. J., Burgess, R. & Marty, B. in *Noble Gases in Geochemistry and Cosmochemistry* Vol. 47 *Reviews in Mineralogy & Geochemistry* (eds D. R. Porcelli, C. J. Ballentine, & R. Weiler) 539-614 (2002).
- 10 Cathles, L. M. & Schoell, M. Modeling CO₂ generation, migration and titration in sedimentary basins. *Geofluids* **7**, 441-450 (2007).
- 11 Baines, S. J. & Worden, R. H. in *Geological Storage of Carbon Dioxide* Vol. 233 *Special Publications* (eds S.J. Baines & R.H. Worden) 59-85 (Geological Society, 2004).
- 12 Xu, S., Nakai, S., Wakita, H., Xu, Y. & Wang, X. Carbon isotopes of hydrocarbons and carbon dioxide in natural gases in China. *Journal of Asian Earth Sciences* **15**, 89-101 (1997).
- 13 Xu, S., Nakai, S., Wakita, H. & Wang, X. Mantle-derived noble gases in natural gases from Songliao Basin, China. *Geochimica et Cosmochimica Acta* **59**, 4675-4683 (1995).
- 14 Ballentine, C. J. & Burnard, P. G. in *Noble Gases in Geochemistry and Cosmochemistry* Vol. 47 *Reviews in Mineralogy & Geochemistry* (eds D. R. Porcelli, C. J. Ballentine, & R. Weiler) 481-538 (2002).
- 15 Ballentine, C. J. & Sherwood Lollar, B. Regional groundwater focusing of nitrogen and noble gases into the Hugoton-Panhandle giant gas field, USA. *Geochimica et Cosmochimica Acta* **66**, 2483-2497 (2002).
- 16 Torgersen, T. & Clarke, W. B. Helium accumulation in groundwater, (i): An evaluation of sources and the continental flux of crustal ⁴He in the Great Artesian Basin, Australia. *Geochimica et Cosmochimica Acta* **49**, 1211-1218 (1985).
- 17 Broadhead, R. F. Natural accumulations of carbon dioxide in the New Mexico region - Where are they, how do they occur and what are the uses for CO₂? *Life Geology* **20**, 2-6 (1998).
- 18 Pearce, J. *et al.* Natural occurrences as analogues for the geochemical disposal of carbon dioxide. *Energy Conversion and Management* **37**, 1123-1128 (1996).
- 19 Kharaka, Y. K. *et al.* Gas-water-rock interactions in Frio Formation following CO₂ injection: Implications for the storage of greenhouse gases in sedimentary basins. *Geology* **34**, 577-580, doi:10.1130/g22357.1 (2006).
- 20 Knauss, K. G., Johnson, J. W. & Steefel, C. I. Evaluation of the impact of CO₂, co-contaminant gas, aqueous fluid and reservoir rock interactions on the geologic sequestration of CO₂. *Chemical Geology* **217**, 339-350 (2005).
- 21 Xu, S., Shun'ichi, N., Wakita, H., Xu, Y. & Wang, X. Helium isotope compositions in sedimentary basins in China. *Applied Geochemistry* **10**, 643-656 (1995).
- 22 Worden, R. H. & Smith, L. K. in *Geological Storage of Carbon Dioxide* Vol. 233 *Special Publications* (eds R. H. Worden & S. J. Baines) 211-224 (Geological Society, London, 2004).
- 23 Xu, S., Nakai, S., Wakita, H., Yongchang, X. & Xianbin, W. Carbon isotopes of hydrocarbons and carbon dioxide in natural gases in China. *Journal of Asian Earth Sciences* **15**, 89-101 (1997).
- 24 Clark, I. D. & Fritz, P. *Environmental Isotopes in Hydrology*. (CRC Press, 1997).
- 25 Deines, P., Langmuir, D. & Harmon, R. S. Stable carbon isotopes and the existence of a gas phase in the evolution of carbonate groundwaters. *Geochimica et Cosmochimica Acta* **38**, 1147 - 1184 (1974).
- 26 Fritz, P. & Fontes, J. C. *Handbook of Environmental Isotope Geochemistry*. Vol. 1. The Terrestrial Environment (Elsevier Scientific Publishing Company, 1980).
- 27 Scharlin, P. *IUPAC Solubility Series 62: Carbon Dioxide in Water and Aqueous Electrolyte Solutions*. (1996).

- 28 Crovetto, R., Fernandez-Prini, R. & Laura Japas, M. Solubilities of inert gases and methane in H₂O and in D₂O in the temperature range of 300 to 600K. *Journal of Chemical Physics* **76**, 1077-1086 (1982).
- 29 Smith, S. P. Noble gas solubility in water at high temperature. *EOS, Transactions of the American Geophysical Union* **66**, 397 (1985).
- 30 Sherwood Lollar, B., O'Nions, R. K. & Ballentine, C. J. Helium and neon isotope systematics in carbon dioxide-rich and hydrocarbon-rich gas reservoirs. *Geochimica et Cosmochimica Acta* **58**, 5279 (1994).

Supplementary Information is linked to the online version of the paper at www.nature.com/nature.

Acknowledgements S.G. was supported by a NERC funded PhD studentship in Manchester and a NERC funded postdoctoral position, grant NE/C516479/1 in Edinburgh and Glasgow, and a UK Energy Research Centre grant NE/C513169/1. Manchester work was further partially funded by NERC grants NE/D004292 and NE/F002823. Toronto work was further partially funded by an NSERC Discovery grant to B.S.L. We extend thanks to all of the field operators for permission to sample the U.S. gas reservoirs and assistance with the background geology, particularly Larry Nugent of BP (Sheep Mountain), Theresa Muhic and Daniel Miller of Iron Creek Energy Group and Gary Grove of Bonanza Creek (McCallum Dome) and Tom White of Rigdeway Petroleum (St. Johns Dome).. S.G. would like to thank Prof. R.S. Haszeldine and Dr. Z. Shipton for supporting this work. Review by R. H. Worden is appreciated.

Author Contributions S.G., C.B. and B.S.L. designed the study, analysed the samples, interpreted the data and wrote the paper. G.H., D.B., Z.D., Z.Z. and G.L.C. assisted with sample analysis and interpretation of the data. S.S., M.S. and M.C. assisted with sample collection and provided comments on the manuscript.

Author Information Reprints and permissions information is available at www.nature.com/reprints. Correspondence and requests for materials should be addressed to S.G. (stuart.gilfillan@ed.ac.uk).

Table 1: Sample location, Producing formation, major gas species and CO₂

carbon isotopes

Field & Well	Location Twnshp-Rnge/Lat-Long	Producing Formation	CO ₂ / ³ He x 10 ⁵	³ He/ ⁴ He (R/R _a)	⁴ He (x 10 ⁻⁴) cm ³ (STP)cm ⁻³	²⁰ Ne (x 10 ⁻⁸) cm ³ (STP)cm ⁻³	δ ¹³ C(CO ₂) ‰
Bravo Dome⁷							
BD01	23/19N/34E	Tubb	4.53 (10)	1.670 (8)	0.944 (12)	0.169 (2)	-3.96 (4)
BD02	32/21N/35E	Tubb	2.25 (5)	0.764 (4)	4.15 (5)	0.700 (7)	-4.93 (8)
BD03	36/22N/34E	Tubb	2.41 (5)	0.896 (4)	3.31 (4)	0.521 (5)	-4.89 (19)
BD04	8/20N/34E	Tubb	4.61 (10)	1.611 (8)	0.961 (2)	0.181 (2)	-4.23 (8)
BD05	34/20N/35E	Tubb	2.74 (6)	0.965 (5)	2.70 (4)	0.446 (4)	-4.95 (5)
BD06	26/22N/32E	Tubb	3.94 (8)	1.503 (8)	1.20 (2)	0.202 (2)	-4.55 (11)
BD07	3/19N/33E	Tubb	4.34 (9)	2.104 (11)	0.781 (10)	0.180 (2)	-4.85 (1)
BD08	9/18N/33E	Tubb	3.87 (8)	1.143 (6)	1.61 (2)	0.264 (3)	-3.88 (8)
BD09	17/21N/33E	Tubb	4.22 (9)	1.724 (9)	0.981 (12)	0.180 (2)	-4.44 (11)
BD10	7/22N/34E	Tubb	3.25 (6)	1.104 (6)	1.99 (3)	0.308 (3)	-4.88 (7)
BD11	25/19N/30E	Tubb	4.82 (10)	3.784 (19)	0.391 (5)	0.103 (1)	-3.66 (29)
BD12	27/19N/30E	Tubb	4.74 (10)	3.627 (18)	0.415 (6)		-3.94 (17)
BD13	22/18N/35E	Tubb	3.54 (8)	1.318 (7)	1.53 (2)	0.240 (3)	-4.42 (3)
BD14	16/18N/34E	Tubb	4.39 (9)	1.413 (7)	1.15 (2)	0.179 (4)	-4.04 (2)
BD12b	27/19N/30E	Tubb	4.75 (10)	3.634 (18)	0.413 (6)	0.120 (2)	-3.94 (17)
McCallum Dome⁷							
No. 3 (8-3)	8/9N/78W	Lakota	1.52 (4)	0.354 (7)	12.3 (2)	1.17 (2)	-5.1 (3)
No. 5	3/9N/79W	Lakota	1.04 (3)	0.409 (7)	15.5 (2)	2.71 (3)	-5.2 (1)
No. 36	8/9N/79W	Dakota/Lakota		0.448 (8)	1.32 (12)	8.10 (8)	nm
No. 13	2/9N/79W	Lakota/Morrison	0.89 (2)	0.393 (7)	18.8 (2)	4.36 (5)	-5.3 (2)
No. 79	4/9N/79W	Dakota/Lakota	1.77 (6)	0.406 (6)	9.16 (21)	2.53 (3)	-5.7 (1)
McElmo Dome⁷							
MC-1	37.4155, -108.7713	Leadville	5.04 (11)	0.145 (2)	9.58 (8)	0.376 (4)	-4.26 (10)
HE-2	37.5052, -108.9094	Leadville	0.68 (15)	0.148 (1)	70.5 (7)	0.307 (30)	-4.40 (10)
YC-4	37.4529, -108.8583	Leadville	4.96 (11)	0.137 (3)	10.2 (10)	0.573 (6)	-4.41 (10)
SC-9	37.3934, -108.8733	Leadville	3.17 (7)	0.150 (3)	14.8 (14)	0.497 (5)	-4.29 (10)
YB-2	37.4472, -108.8075	Leadville	8.74 (20)	0.125 (1)	6.42 (61)	0.371 (4)	-4.40 (10)
YC-1	37.4529, -108.8583	Leadville	4.07 (9)	0.142 (2)	12.1 (12)	0.423 (5)	-4.34 (10)
HF-1	37.4871, -108.8807	Leadville	2.16 (6)	0.169 (1)	19.3 (26)	0.564 (12)	-4.37 (10)
HD-2	37.4572, -108.9008	Leadville	4.28 (10)	0.140 (3)	11.7 (12)	0.128 (2)	-4.38 (10)
YA-2	37.4692, -108.7811	Leadville	3.39 (8)	0.138 (3)	15.0 (15)	0.130 (2)	-4.42 (10)
YE-1	37.4818, -108.8123	Leadville	4.16 (9)	0.173 (3)	9.75 (8)	0.143 (3)	-4.45 (10)
HA-1	37.5289, -108.8718	Leadville	4.56 (10)	0.139 (3)	11.0 (11)	0.205 (7)	-4.66 (10)
SC-10	37.3934, -108.8733	Leadville	4.37 (10)	0.139 (2)	11.6 (11)	0.413 (5)	-4.27 (10)
HC-2	37.4734, -108.8860	Leadville	4.68 (11)	0.140 (2)	10.7 (10)	0.409 (5)	-4.38 (10)
HB-1	37.5087, -108.8802	Leadville	4.74 (11)	0.148 (3)	9.94 (10)	0.247 (4)	-4.49 (10)
YD-1	37.4619, -108.8224	Leadville	8.50 (20)	0.145 (3)	5.68 (6)	0.366 (5)	-4.46 (10)
JM Brown Basset⁵							
Turk State No. 1A	30.38758, -101.85642	Ellenberger	5.92 (47)	0.543 (16)	1.25 (9)	nm	-2.88
Bassett Goode No. 3	30.37852, -101.83068	Ellenberger	5.55 (43)	0.527 (16)	1.42 (10)	nm	-2.89
Brown Bassett No. 2*	30.34433, -101.7995	Ellenberger	5.82 (35)	0.502 (15)	1.33 (7)	nm	-2.90
Mayne K. Martin ETAL 1	30.35661, -101.74721	Ellenberger	5.29 (40)	0.372 (11)	1.42 (10)	nm	-2.97
Mitchell 109 No. 2*	30.33329, -101.69826	Ellenberger	4.58 (36)	0.400 (12)	1.53 (11)	nm	-2.92
Mitchell 5 No. 1X	30.32352, -101.68429	Ellenberger	5.61 (43)	0.478 (11)	1.40(10)	nm	-2.84
Mitchell 103 No. 2	30.3568, -101.63642	Ellenberger	4.20 (33)	0.246 (7)	1.39 (10)	nm	-2.70
Mitchell No. 6	30.351, -101.58835	Ellenberger	3.93 (31)	0.264 (8)	1.51 (11)	nm	-2.96
Mitchell No. 3	30.33966, -101.61307	Ellenberger	4.22 (33)	0.240 (7)	1.39 (10)	nm	-3.06
Mitchell A-11 No. 1	30.30286, -101.57677	Ellenberger	4.07 (32)	0.272 (8)	1.66 (12)	nm	-2.93
Mitchell No. 12	30.29118, -101.57295	Ellenberger	4.24 (130)	0.267 (8)	1.46 (10)	nm	-2.96
Sheep Mountain⁷							
8-2-P	2/9-28S/70W	Dakota	2.31 (5)	0.981 (10)	3.13 (3)	1.47 (2)	-5.0 (2)
2-10-O	15/9-27S/70W	Entrada	2.44 (6)	0.984 (12)	2.96 (3)	3.04 (3)	-5.2 (1)
9-26	26/9-27S/70W	Dakota	2.57 (6)	0.934 (14)	2.95 (3)	0.613 (9)	nm
2-9-H	9/9-27S/70W	Dakota	2.44 (6)	0.945 (19)	3.07 (3)	9.77 (10)	nm
3-15-B	15/9-27S/70W	Dakota	2.61 (6)	0.937 (16)	2.90 (3)	1.54 (2)	-5.7 (4)
4-13		Dakota	2.17 (5)	0.942 (18)	3.47 (4)	1.11 (2)	nm
4-26-E	26/9-27S/70W	Entrada	2.20 (5)	1.024 (18)	3.15 (3)	0.442 (4)	-4.8 (1)
3-23-D	22/9-27S/70W	Dakota	2.26 (5)	0.988 (14)	3.17 (3)	0.579 (9)	nm
7-35-L	2/9-28S/70W	Dakota	2.53 (6)	0.916 (14)	3.06 (3)	0.749 (12)	-5.0 (2)
2-35-C	26/9-27S/70W	Dakota	2.57 (6)	0.963 (19)	2.87 (3)	0.573 (8)	nm
1-15-C	15/9-27S/70W	Entrada	2.71 (6)	0.967 (16)	2.71 (3)	6.77 (10)	nm
3-4-O	9/9-27S/70W	Dakota	2.53 (6)	0.937 (14)	2.99 (3)	2.64 (3)	-5.8 (3)
4-14-M	22/9-27S/70W	Dakota	2.65 (6)	0.892 (15)	3.00 (3)	1.11 (1)	nm
5-15-O	22/9-27S/70W	Dakota	2.30 (5)	1.056 (15)	2.92 (3)	4.33 (5)	-5.0 (1)

Field & Well	Location Twnshp-Rnge/Lat-Long	Producing Formation	CO ₂ / ³ He x 10 ⁹	³ He/ ⁴ He (R/R _a)	⁴ He (x 10 ⁻⁴) cm ³ (STP)cm ⁻³	²⁰ Ne (x 10 ⁻⁸) cm ³ (STP)cm ⁻³	δ ¹³ C(CO ₂) ‰
Sheep Mountain ⁷			2.90 (7)				
4-4-P	9/9-27S/70W	Dakota		0.970 (14)	2.52 (2)	1.31 (2)	nm
5-9-A	9/9-27S/70W	Dakota	2.39 (6)	1.006 (18)	2.94 (3)	1.28 (2)	nm
1-1-J	2/9-28S/70W	Dakota	3.61 (8)	0.908 (16)	2.16 (2)	0.878 (12)	-5.2 (1)
1-22-H	22/9-28S/70W	Entrada	2.25 (5)	0.981 (17)	3.22 (3)	0.937 (13)	-4.5 (2)
St. Johns Dome ⁷							
22-1X	34.4265, -109.2664	Supai	0.098 (2)	0.455 (8)	134 (13)	34.4 (47)	-3.65 (5)
10-22	34.2437, -109.1645	Supai	1.91 (42)	0.394 (8)	9.42 (9)	2.30 (4)	-3.79 (5)
3-1	34.3771, -109.2563	Supai	0.22 (3)	0.433 (9)	70.6 (7)	15.1 (21)	-3.85 (5)
Jilllin Field ^{12, 13, 23}							
Wan 2		Cretaceous	1.44 (4)	4.91 (6)	1.00 (2)	nm	-3.6
Wan 5		Cretaceous	227 (7)	4.10 (4)	0.0076 (2)	0.0547 (15)	-5.0
Wan 6		Cretaceous	8.32 (3)	4.99 (5)	0.169 (4)	0.230 (6)	-3.8
Wan 8		Cretaceous	nm	4.30 (5)	nm	nm	-3.2
Wan 9		Cretaceous	36.6 (10)	4.08 (4)	0.047 (1)	0.130 (3)	-3.8
Subai Basin ^{12, 23}							
Huangqyan 1		Permian	2.17 (7)	3.52 (5)	3.13 (3)	1.47 (2)	-3.6
Sutail 74		Devonian	0.493(14)	3.59 (4)	2.96 (3)	3.04 (3)	-4.1
Su203		Eocene	0.459 (13)	2.61 (3)	2.95 (3)	0.613 (9)	-2.7
Kismarja ^{8,30}							
Kismarja 8		Up. Pannonian	20.2 (5)	1.33 (3)	0.226 (7)	nm	-5.0
Kismarja 79		Up. Pannonian	15.5 (4)	1.38 (3)	0.310 (10)	nm	-4.9
Kismarja 61		Up. Pannonian	27.3 (6)	1.16 (2)	0.205 (6)	nm	-5.1
Kismarja 55		Up. Pannonian	13.3 (3)	1.38 (3)	0.360 (11)	nm	-5.1
Kismarja 56		Up. Pannonian	1090 (3)	1.16 (2)	0.0052 (2)	nm	-6.8
Kismarja 74		Up. Pannonian	65.2 (2)	1.34 (3)	0.078 (3)	nm	-6.4
Kismarja 22		Up. Pannonian	1.52 (1)	1.02 (2)	1.31 (3)	nm	-6.6

nm = not measured

1σ error shown in brackets

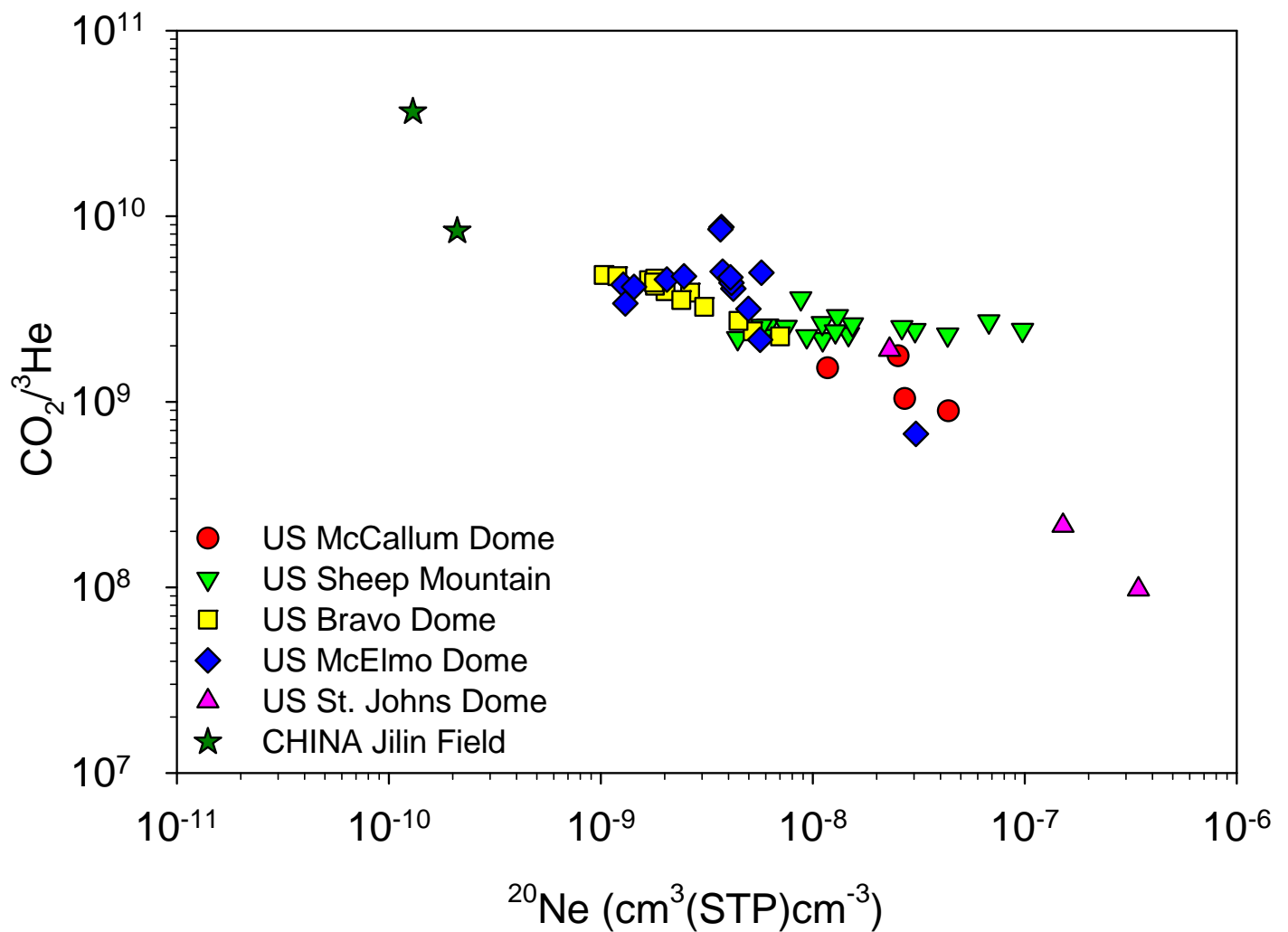
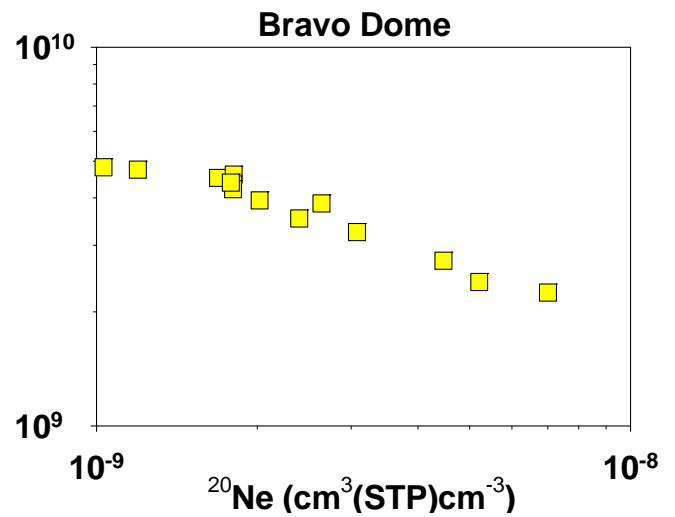
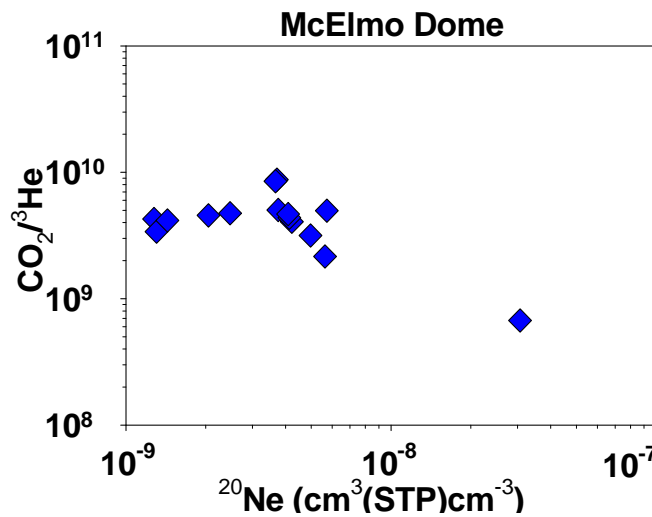
Figure Captions

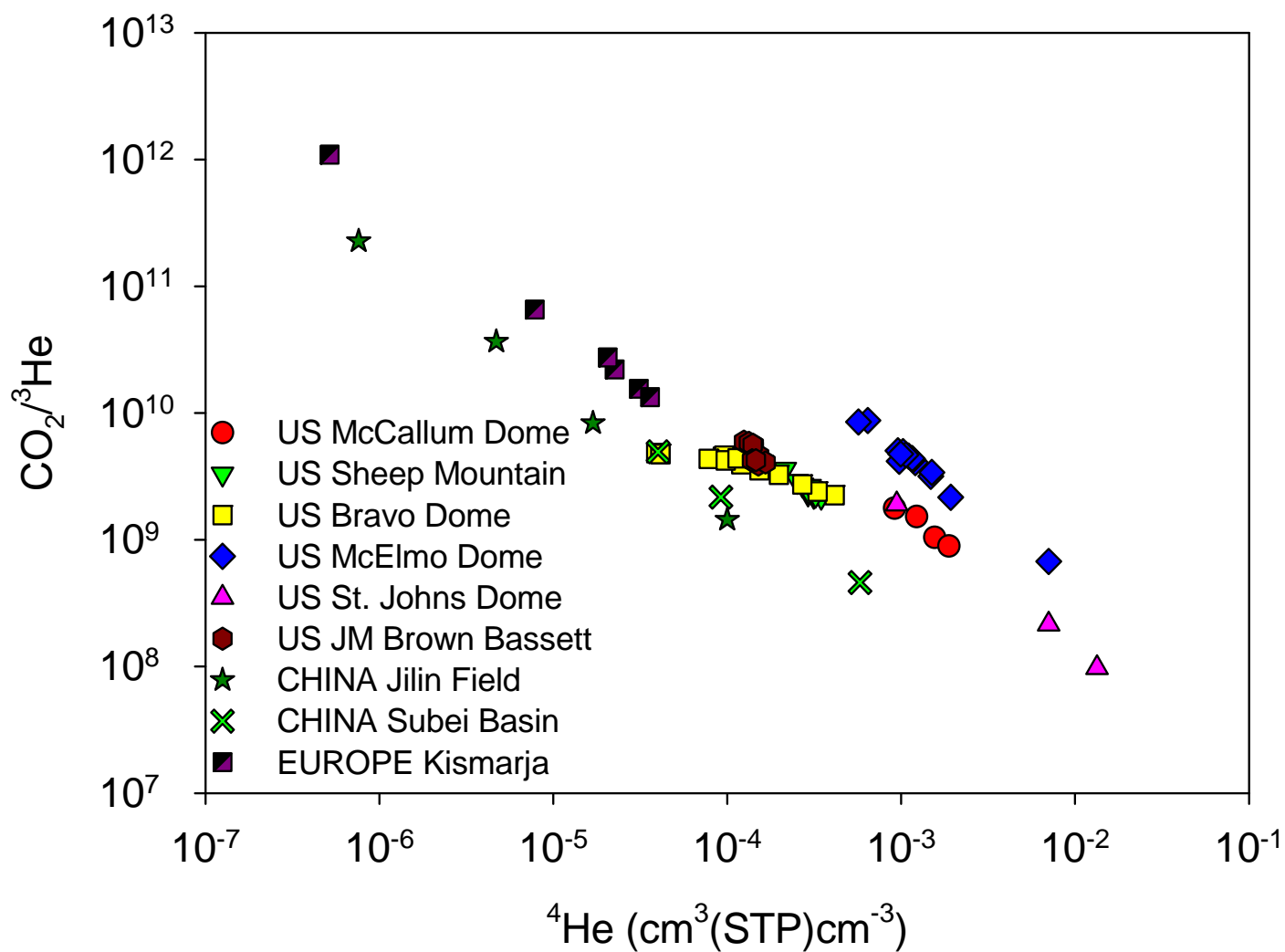
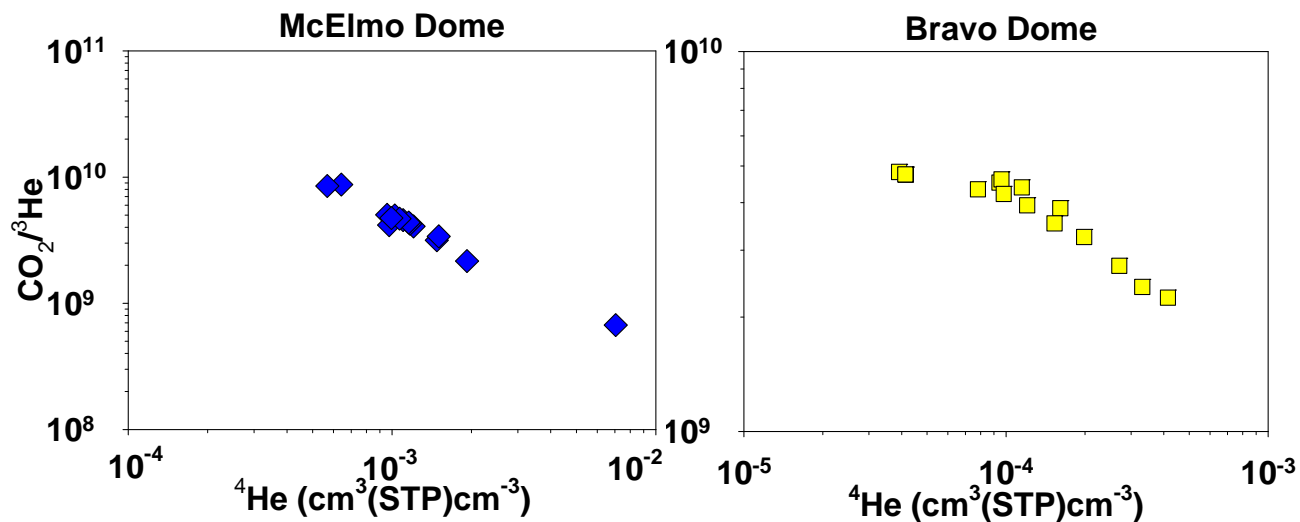
Figure 1. $\text{CO}_2/{}^3\text{He}$ variation plotted against ${}^{20}\text{Ne}$ in samples from the ‘global’ data set of CO_2 -rich natural gas fields (see text). There is a general trend in this data set of decreasing $\text{CO}_2/{}^3\text{He}$ with increasing ${}^{20}\text{Ne}$. This trend is most clearly apparent in the siliciclastic case type Bravo Dome data set (inset) but less clear in the carbonate case type reservoir, McElmo Dome (inset). ${}^3\text{He}$ is conservative within the gas phase. Lower $\text{CO}_2/{}^3\text{He}$ therefore represent subsurface reduction in CO_2 concentration in the emplaced CO_2 phase. Since the only subsurface source of the ${}^{20}\text{Ne}$ now in the CO_2 phase is the formation water, the CO_2 sink must be linked to the formation water contacted by the gas phase.

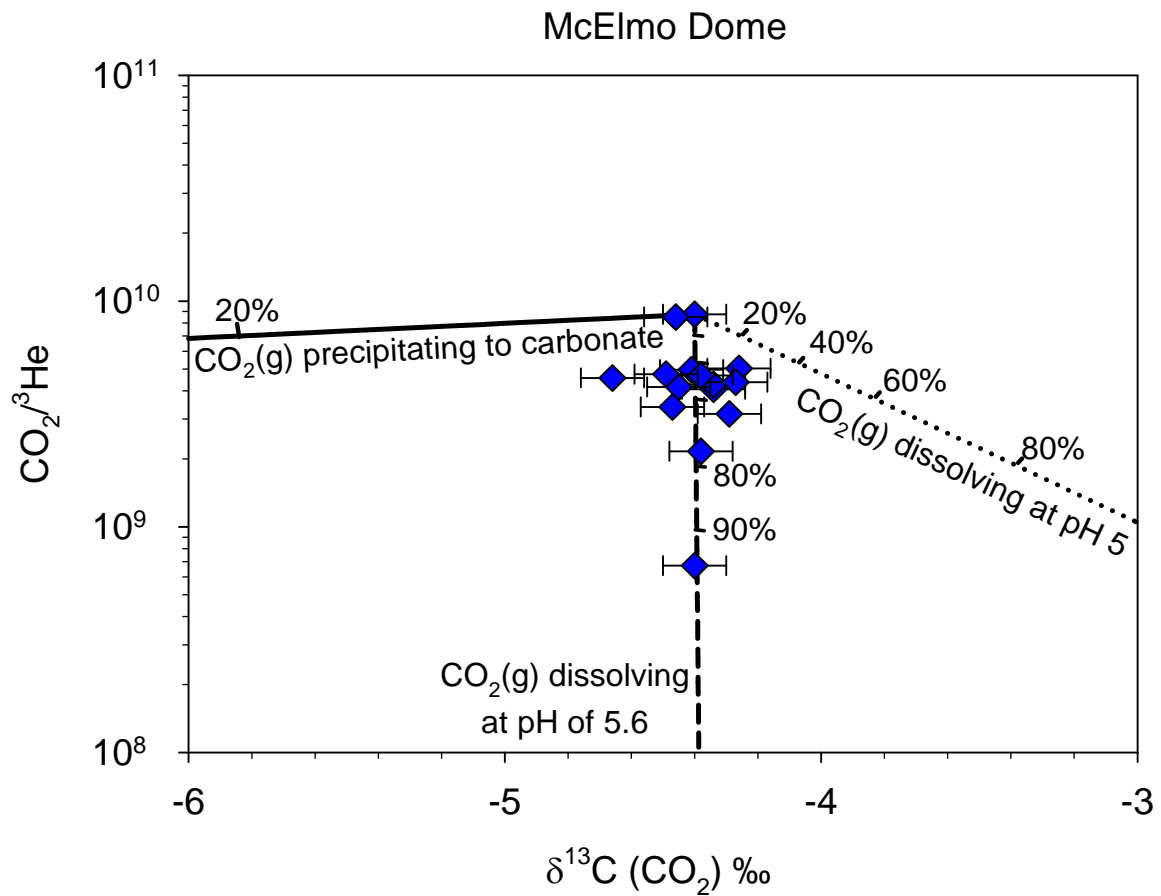
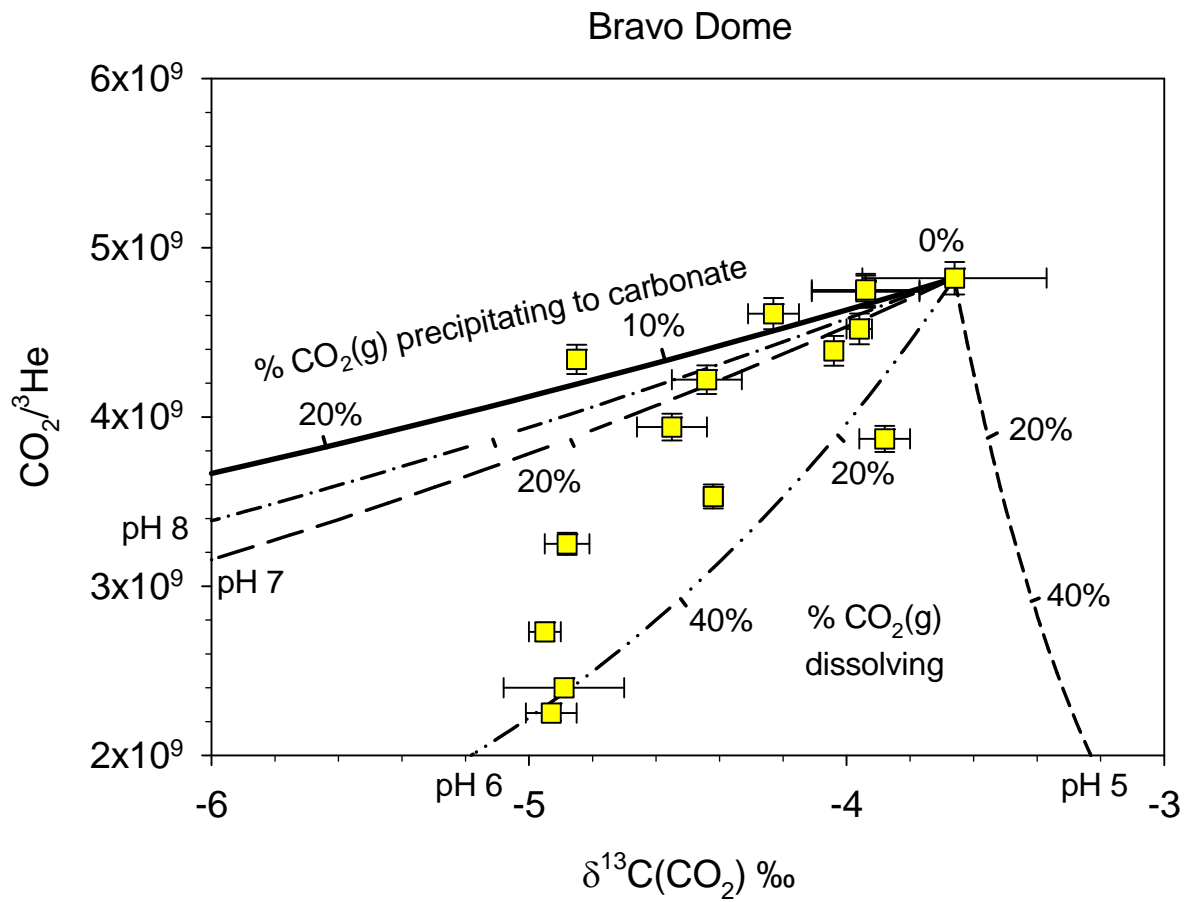
Figure 2. The ‘global’ data sets of CO_2 gas fields also show a strong correlation between decreasing $\text{CO}_2/{}^3\text{He}$ and increasing ${}^4\text{He}$ concentration. ${}^4\text{He}$ accumulates in formation water over time^{7,15,16} and underscores the importance of formation water in controlling the mechanism of subsurface CO_2 removal (Fig.1 and text). We speculate that the formation water ${}^4\text{He}$ signature with $\text{CO}_2/{}^3\text{He}$ is more coherent than the ${}^{20}\text{Ne}$ (Fig. 1) due to perturbation of ${}^{20}\text{Ne}$ in ancient formation water through non-water phase interaction⁹ with subsequent ${}^4\text{He}$ accumulation providing a homogenous regional scale formation water ${}^4\text{He}$ signal^{15,16}. Different $\text{CO}_2/{}^3\text{He}$ vs. ${}^4\text{He}$ gradients will be due to different local formation water ${}^4\text{He}$ accumulation rates.

Figure 3. $\delta^{13}\text{C}(\text{CO}_2)$ against $\text{CO}_2/{}^3\text{He}$ for Bravo Dome (Top) and McElmo Dome (Bottom) Error bars are 1σ . Top Panel: The solid line shows the predicted trend for carbonate mineral precipitation and the dashed lines show $\text{CO}_2(\text{g})$ dissolution trends

for varying formation water pH (see methods). Bravo Dome data is not consistent with the major CO₂ sink being precipitation of carbonate (see text). Bottom Panel: Invariant $\delta^{13}\text{C}(\text{CO}_2)$ with over an order of magnitude change in CO₂/³He in McElmo Dome gases cannot be accounted for by precipitation (solid line). Dissolution of reservoir CO₂ into formation water at pH=5.6 would produce the observed results (see text).







Supplementary Information:

Supplementary Table 1
Reservoir Conditions Used in Models

Reservoir	Average Well Depth (m)	Pressure (MPa)	Borehole Temperature (K)	TDS (molar)	K _{He} (GPa)	K _{CO2} (GPa)	Fractionation (1000ln α) for CO _{2(g)} forming (‰) [24]		
							H ₂ CO _{3(aq)}	HCO ₃ ⁻	CaCO ₃
Bravo Dome ³⁰	820	8.03	314	1.45	20.1	0.349	-0.846	6.63	8.55
JM Brown Bassett ⁹	2800*	27.4*	373	1.00*	14.0	0.774	-0.864	3.36	4.96
McCallum Dome ⁷	1630	16.0	338	0.228	14.1	0.460	-0.854	5.10	6.85
McElmo Dome ⁷	2450	24.0	344	0.200	11.9	0.487	-0.856	4.76	6.48
Sheep Mountain ⁷	1400	13.7	331	0.0137	13.6	0.438	-0.852	5.51	7.29
St. Johns Dome ³¹	630	6.17	322	0.0720	14.4	0.281	-0.849	6.08	7.92
Jilin Field ²¹	840	8.23	333*	1.00*	17.4	0.491	-0. 853	5.39	7.16
Subei Basin ¹²	2251	22.1	357*	1.00*	15.4	0.665	-0.860	4.09	5.75
Kismarja ²⁹	825	8.08	326*	1.00*	17.7	0.438	-0.850	5.82	7.63

*JM Brown Bassett depth estimated from bottom hole temperature and 30°C/km geothermal gradient. Jilin Field, Subei Basin and Kismarja borehole temperatures estimated from depth and geothermal gradient. JM Brown Bassett, Jilin Field, Subei Basin and Kismarja salinity estimated.

Additional References for Supplementary Table

30. Broadhead, R. F. Carbon dioxide in northeast New Mexico. *West Texas Geological Society Bulletin* **32**, 5-8 (1993).
31. Stevens, S. H., Fox, C., White, T. & Melzer, S. Natural CO₂ analogs for Carbon Sequestration. *Final Report for USDOE* (2006).